

Effect of Thickness and Phosphorus Content on Au/Pd/Ni(P) Metal Finish of Printed Circuit Board

CHIH-KAI HUANG,¹ KEH-WEN LIN,² YU-MING HUANG,²
ALVIN R. CAPARANGA,^{1,3} RHODA B. LERON,¹ and MENG-HUI LI^{1,4}

1.—Department of Chemical Engineering and R&D Center for Membrane Technology, Chung Yuan Christian University, Chung Li City 32023, Taiwan, ROC. 2.—OMG (Asia) Electronics Company Limited, Chung Li City 32053, Taiwan, ROC. 3.—School of Chemical Engineering and Chemistry, Mapúa Institute of Technology, Intramuros, 1002 Manila, Philippines. 4.—e-mail: mhli@cycu.edu.tw

Electroless nickel/electroless palladium/immersion gold [Au/Pd/Ni(P) or ENEPIG] pads consisting of layers of Ni(P) (200 μin), pure palladium (Pd) or palladium phosphorus (PdP) (2 μin , 4 μin or 6 μin), and gold (Au) (2 μin or 4 μin) were prepared using two different processes (wire bonding and lead-free soldering). Each of these processes was done with zero- or two-time reflow. Different tests on solderability, wettability, wire-bonding capacity, and corrosion resistance were performed on different combinations of ENEPIG pads formed using different combinations of processes and conditions. Scanning electron microscopy was also performed to examine the surface characteristics of the pads. It was found that the ENEPIG pad sample with the 4- μin -thick Au and 4- μin -thick PdP layers possessed stable wire-bonding capacity and excellent lead-free solder reliability. In addition, the ENEPIG–PdP systems showed better corrosion resistance, which is attributed to the presence of the amorphous PdP layer protecting the nickel layer.

Key words: ENEPIG, PCB, corrosion, wire bonding, lead-free soldering

INTRODUCTION

Of the five types of metal finish used on printed circuit board (PCB) in the electronics industry—hot-air solder level, immersion tin, immersion silver, organic solderability preservatives, and electroless nickel/immersion gold [Au/Ni(P) or ENIG]—the last one (ENIG) has been the most widely used. However, the immersion gold process has been reported to cause corrosion on the nickel layer (i.e., oxidation of Ni^0 by Au^{2+}), resulting in the formation of so-called *black pads*.^{1–5} The black-pad defect is problematic because it can result in solder joint failure and low shear strength after assembly. Nonetheless, after understanding the black-pad phenomenon and the virtual elimination of black-pad defects, the ENIG process still persisted.⁶

Recently, however, the electroless nickel/electroless palladium/immersion gold [Au/Pd/Ni(P) or ENEPIG] process has provided an alternative to ENIG. This can improve the stability of the wire-bonding process, and can limit Ni(P) corrosion by depositing a Pd layer over the Ni layer (i.e., between Ni and Au bilayers)^{7,8} to prevent oxidation of Ni^0 by Au^{2+} . In addition to all the advantages of the ENIG process,⁹ the ENEPIG process offers the following advantages: thinner Au layer, flat pad surface, excellent shelf life, good contact connection of pad, excellent lead-free solder reliability, stable wire-bonding capacity, and prevention of formation of black pads.^{7,10} In this study, we investigated the effects on the properties of ENEPIG metal finish of the following: presence of phosphorus (P) in the Pd layer, thickness of Pd layer, thickness of Au layer, and aging [i.e., heating by infrared (IR) reflow oven]. The investigated properties of the metal finish were wettability, solderability, wire-bonding capacity, and corrosion resistance.

(Received August 17, 2012; accepted April 13, 2013;
published online May 25, 2013)

EXPERIMENTAL PROCEDURES

ENEPIG Metal Finish

The type of surface finish investigated in the study was ENEPIG with varied combinations of thickness of pure palladium (Pd) or palladium-phosphorus (PdP) ($2\text{ }\mu\text{in}$, $4\text{ }\mu\text{in}$, and $6\text{ }\mu\text{in}$) and Au ($2\text{ }\mu\text{in}$ and $4\text{ }\mu\text{in}$) layers following a $200\text{-}\mu\text{in}$ Ni(P) layer. The ENEPIG process (Fig. 1) is similar to the ENIG process¹¹ with an additional step involving the deposition of electroless Pd (EP) between the electroless Ni (EN) deposition and immersion Au (IG) steps.

Tests

The following tests were performed on ENEPIG metal surface finishes (with different thicknesses of Pd and Au layers).

Wettability

The surface wettability of each sample was determined by measuring the solder spread length, wetting time, and wetting force. The procedure for determining solder spread length involved cleaning the surface (using methanol), coating it with flux, and melting a tin ball on the sample surface by heating it in an oven (with or without reflow). The tin ball used was made of lead-free solder (Sn96.5-Ag3-Cu0.5, SAC305). The reflow profile of the oven (with reflow) is shown in Fig. 2. After heating, the spread length of the melted tin ball was then measured. Wetting force and wetting time, on the other hand, were determined using a wetting balance (MUST System II PLUS).

Mechanical Strength

Solderability and wire bond strength are indicative of a metal surface finish's mechanical strength. Two standard tests were performed to quantify the solderability of the metal surface finishes: ball shear strength (DAGE series 4000: test speed $500\text{ }\mu\text{m/s}$,

test load 200 g, shear height $10\text{ }\mu\text{m}$) and cold ball pull strength (DAGE series 4000: test speed $500\text{ }\mu\text{m/s}$, test load 410 g). In both tests, SAC305 solder (tin ball) was used. Wire bond strength was determined using the standard wire bond pull test (K&S 1488 Plus gold wire ball bonder: test load $2000\text{ }\mu\text{m/s}$, test load 4.00 g).

Surface Characteristics

Scanning electron microscopy (SEM, S-3400N; Hitachi) was used to analyze the surface characteristics of the pads.

RESULTS AND DISCUSSION

Wettability

The wettability of a metal surface finish is indicative of its solderability. One wettability test done in this study was the determination of the spread length of the solder. The results of this test are presented in Table I. Results suggest that the spread length was practically independent of the Pd or PdP layer thickness. However, the metal finish with a Pd layer was observed to exhibit longer solder spread length than the metal finish with a PdP layer. The presence of phosphorus could have stalled the extent of the spread. A thicker Au layer ($4\text{ }\mu\text{in}$ versus $2\text{ }\mu\text{in}$) would mean a shorter spread length, as suggested by the results. Despite these

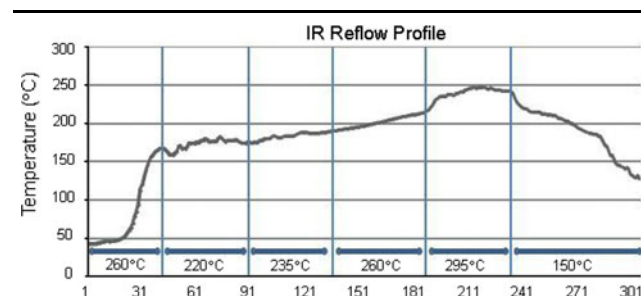


Fig. 2. SMD hot air reflow profile.

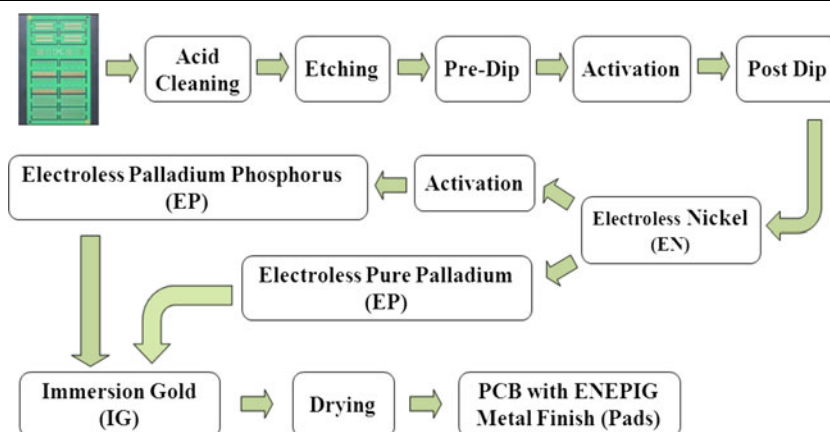


Fig. 1. ENEPIG process.

individual effects of the thicknesses of the phosphorus and Au layers, all the measured solder spread lengths were indicative of good solderability of the samples.

Wetting force was measured using a wetting balance. As shown in Table II, all measured wetting forces (from minimum to maximum) were greater than 0, indicating that all the surfaces exhibited wettability. However, the wetting force measurement values were practically similar (or equal), as suggested by the statistically identical minimum, maximum, mean, and standard deviation values. This means that the Au layer thickness and P content did not have significant effects on the maximum wetting force for all samples. Wetting time, on the other hand, should be less than the standard 0.6 s for the metal surface finish to be considered to have good wetting characteristics. All mean values of wetting time for all samples (Table III) were less than 0.6 s, meaning that any combination of Pd/PdP and Au layer thicknesses resulted in a metal surface finish with good wettability. However, there were individual maximum values that were higher than 0.6 s; such values are presented in italics in Table III. Samples with $t_0 > 0.6$ s failed this test. This particular test gave results that seemed to suggest generally good and acceptable wetting times for samples with 4- μin and 6- μin PdP layers regardless of the Au layer thickness and manner of aging (with 2 \times or without reflow).

Values of $t_{2/3}$ should be not more 1 s for the surface to be considered to have good wettability. There were instances in which, for several samples tested, values of $t_{2/3}$ were greater than 1 s. It can be deduced from Table IV that better values of $t_{2/3}$ were obtained as the Pd layer thickness increased. Between pure Pd and PdP, the latter gave better values of $t_{2/3}$.

In summary, ENEPIG–PdP systems had better wettability than ENEPIG–Pd systems. In case of no aging, the increase in the Au layer thickness resulted in a decreased number of samples that failed the $t_{2/3}$ test, but had no effect on the number of samples that failed the t_0 test. In the case of aging

with 2 \times reflow, the increase in the Au layer thickness resulted in an increase in the number of samples that failed both t_0 and $t_{2/3}$ tests.

Mechanical Strength

For each type of ENEPIG, 270 samples were tested for ball shear strength. The results (Table V) suggest that the ENEPIG–Pd samples with a 2- μin or 4- μin Au layer had ball shear strength values that were practically the same. Also, in all instances, the ENEPIG samples with PdP had shear strength values that were lower than those of the ENEPIG–Pd samples. It can be theorized that such results can be attributed to the crystal structures of the Pd and PdP deposits. Some studies reported that PdP deposit on nickel surface has an amorphous structure while Pd deposit has a fine crystalline structure.^{12,13} The stability of the latter could have caused the ENEPIG–Pd systems to have higher ball shear strength than the ENEPIG–PdP systems. It is also important to note that, for the ENEPIG–PdP samples, the shear strength decreased with increasing PdP layer thickness. However, all such values were better than the acceptable standard shear force of 1000 g.

In the cold ball pull test, 40 samples were tested for every type of ENEPIG. The cold ball pull strength values for the samples are also presented in Table V. In all instances, the cold ball pull strength values decreased with increasing Au layer thickness, and the values were higher for ENEPIG–Pd than for ENEPIG–PdP samples. These observations uphold the observations gathered in the ball shear strength test. More important to note, however, would be the failure modes (associated with the cold ball pull strength test) of the ENEPIG samples subjected to this test. Such failure mode mechanisms are presented in the SEM micrographs in Fig. 3 as follows: pad before test (Fig. 3a); ball failure (Fig. 3b), the preferred failure mode occurs mostly within the solder ball; pad failure (Fig. 3c), the bond of the solder ball to the pad is stronger than the pad-to-substrate adhesive strength; and

Table I. Solder spread length of ENEPIG–Pd and ENEPIG–PdP with varying thicknesses of Pd (or PdP) and Au layers

| System | Pd or PdP Layer Thickness (μin) | Solder Spread Length (mm) | |
|------------|--|---------------------------|----------------------|
| | | 2- μin Au | 4- μin Au |
| ENEPIG–Pd | 2 | 5.773 \pm 0.614 | 7.068 \pm 0.899 |
| | 4 | 5.796 \pm 0.766 | 7.123 \pm 0.639 |
| | 6 | 5.763 \pm 0.540 | 6.693 \pm 0.399 |
| ENEPIG–PdP | 2 | 5.262 \pm 0.871 | 6.898 \pm 0.709 |
| | 4 | 5.298 \pm 0.700 | 6.889 \pm 0.663 |
| | 6 | 5.265 \pm 0.687 | 6.653 \pm 0.369 |

No. of samples = 16; no. of pads per sample = 4

Table II. Maximum wetting force (F_{\max}) of ENEPIG–Pd and ENEPIG–PdP with varying thicknesses of Pd (or PdP) and Au layers and reflow time at fixed Ni layer thickness

| System | Maximum Wetting Force (mN) (No Reflow) | | | | Maximum Wetting Force (mN) (with 2× Reflow) | | | |
|----------------------|--|------|------|-----------|---|------|------|-----------|
| | Max. | Min. | Mean | Std. Dev. | Max. | Min. | Mean | Std. Dev. |
| Ni(200)/Pd(2)/Au(2)* | 2.99 | 2.29 | 2.69 | 0.17 | 2.89 | 2.24 | 2.60 | 0.18 |
| Ni(200)/Pd(4)/Au(2) | 2.92 | 2.23 | 2.64 | 0.19 | 2.99 | 2.34 | 2.60 | 0.15 |
| Ni(200)/Pd(6)/Au(2) | 2.95 | 2.24 | 2.64 | 0.21 | 2.94 | 2.36 | 2.59 | 0.14 |
| Ni(200)/Pd(2)/Au(4) | 3.02 | 2.38 | 2.77 | 0.16 | 2.94 | 2.35 | 2.66 | 0.15 |
| Ni(200)/Pd(4)/Au(4) | 3.02 | 2.43 | 2.68 | 0.16 | 2.89 | 2.39 | 2.65 | 0.13 |
| Ni(200)/Pd(6)/Au(4) | 2.87 | 2.37 | 2.65 | 0.14 | 2.92 | 2.36 | 2.60 | 0.15 |
| Ni(200)/PdP(2)/Au(2) | 2.88 | 2.13 | 2.52 | 0.20 | 2.94 | 2.31 | 2.56 | 0.15 |
| Ni(200)/PdP(4)/Au(2) | 2.87 | 2.19 | 2.56 | 0.18 | 2.88 | 2.28 | 2.62 | 0.14 |
| Ni(200)/PdP(6)/Au(2) | 2.89 | 2.26 | 2.58 | 0.17 | 2.89 | 2.32 | 2.60 | 0.13 |
| Ni(200)/PdP(2)/Au(4) | 2.88 | 2.25 | 2.61 | 0.16 | 2.93 | 2.31 | 2.63 | 0.17 |
| Ni(200)/PdP(4)/Au(4) | 2.86 | 2.27 | 2.56 | 0.15 | 2.97 | 2.29 | 2.64 | 0.15 |
| Ni(200)/PdP(6)/Au(4) | 2.87 | 2.20 | 2.50 | 0.17 | 2.85 | 2.24 | 2.59 | 0.15 |

*Values in parentheses indicate the thickness (μin) of the respective metal layer; standard wetting force > 0 mN; no. of samples = 14; no. of pads per sample = 3

Table III. Wetting time (t_0) of ENEPIG–Pd and ENEPIG–PdP with varying thicknesses of Pd (or PdP) and Au layers and reflow time at fixed Ni layer thickness

| System | Wetting Time (s) (No Reflow) | | | | Wetting Time (s) (with 2× Reflow) | | | |
|----------------------|------------------------------|-------|-------|-----------|-----------------------------------|-------|-------|-----------|
| | Max. | Min. | Mean | Std. Dev. | Max. | Min. | Mean | Std. Dev. |
| Ni(200)/Pd(2)/Au(2)* | 0.623 | 0.003 | 0.113 | 0.175 | 0.858 | 0.003 | 0.201 | 0.249 |
| Ni(200)/Pd(4)/Au(2) | 0.385 | 0.003 | 0.100 | 0.119 | 0.603 | 0.003 | 0.153 | 0.192 |
| Ni(200)/Pd(6)/Au(2) | 0.420 | 0.003 | 0.165 | 0.165 | 0.603 | 0.003 | 0.172 | 0.187 |
| Ni(200)/Pd(2)/Au(4) | 0.603 | 0.003 | 0.266 | 0.186 | 1.261 | 0.003 | 0.372 | 0.291 |
| Ni(200)/Pd(4)/Au(4) | 0.336 | 0.003 | 0.145 | 0.103 | 1.032 | 0.003 | 0.253 | 0.299 |
| Ni(200)/Pd(6)/Au(4) | 0.351 | 0.003 | 0.115 | 0.140 | 0.819 | 0.003 | 0.152 | 0.217 |
| Ni(200)/PdP(2)/Au(2) | 0.595 | 0.003 | 0.183 | 0.205 | 0.696 | 0.003 | 0.193 | 0.196 |
| Ni(200)/PdP(4)/Au(2) | 0.405 | 0.003 | 0.126 | 0.134 | 0.455 | 0.003 | 0.130 | 0.142 |
| Ni(200)/PdP(6)/Au(2) | 0.368 | 0.003 | 0.112 | 0.122 | 0.429 | 0.003 | 0.116 | 0.149 |
| Ni(200)/PdP(2)/Au(4) | 0.411 | 0.003 | 0.103 | 0.138 | 0.639 | 0.003 | 0.165 | 0.178 |
| Ni(200)/PdP(4)/Au(4) | 0.486 | 0.003 | 0.141 | 0.166 | 0.492 | 0.003 | 0.152 | 0.160 |
| Ni(200)/PdP(6)/Au(4) | 0.510 | 0.003 | 0.127 | 0.147 | 0.558 | 0.003 | 0.122 | 0.149 |

*Values in parentheses indicate the thickness (μin) of the respective metal layer; standard $t_0 \leq 0.6$ s; no. of samples = 14; no. of pads per sample = 3

bond failure (Fig. 3d), indicating brittle failure. For the samples tested in this study, only bond failure, pad failure, and ball failure were observed (Figs. 4, 5). The ball failure mode accounted for more than 80% of the observed failures, which is a favorable result. However, the bond failure mode seemed to be affected by the Au layer thickness. For the ENEPIG–Pd samples with a 2- μin Au layer, an increase in the Pd layer thickness resulted in a decrease in the percentage of bond failure modes observed. The opposite trend was observed for ENEPIG–Pd samples with a 4- μin Au layer. For the ENEPIG–PdP samples with a 2- μin or 2- μin Au

layer, the percentages of bond failure mode for the pads with a 4- μin PdP layer were lower than those with the 2- μin or 6- μin PdP layers.

In the wire bond pull test, 400 samples were tested for each type of ENEPIG. The wire bond pull strengths of ENEPIG–Pd and ENEPIG–PdP with a 2- μin Au layer and varying thickness of Pd or PdP layer and reflow time are shown in Fig. 6. The samples with a 2- μin Pd (or PdP) layer had a wider range of wire bond pull strength values than the samples with a 4- μin or 6- μin Pd (or PdP) layer. The wire bond pull strength values for the pads that were aged with 2× reflow were generally lower than

Table IV. Time for the wetting curve to reach two-thirds of the maximum wetting force ($t_{2/3}$) for ENEPIG-Pd and ENEPIG-PdP with varying thicknesses of Pd (or PdP) and Au layers and reflow time at fixed Ni layer thickness

| System | $t_{2/3}$ (s) (No Reflow) | | | | $t_{2/3}$ (s) (with 2× Reflow) | | | |
|----------------------|---------------------------|------|------|-----------|--------------------------------|------|------|-----------|
| | Max. | Min. | Mean | Std. Dev. | Max. | Min. | Mean | Std. Dev. |
| Ni(200)/Pd(2)/Au(2)* | 1.64 | 0.22 | 0.54 | 0.40 | 1.87 | 0.25 | 0.58 | 0.37 |
| Ni(200)/Pd(4)/Au(2) | 1.17 | 0.23 | 0.49 | 0.25 | 1.43 | 0.23 | 0.51 | 0.30 |
| Ni(200)/Pd(6)/Au(2) | 1.13 | 0.22 | 0.54 | 0.25 | 1.39 | 0.23 | 0.54 | 0.32 |
| Ni(200)/Pd(2)/Au(4) | 1.37 | 0.18 | 0.61 | 0.30 | 2.59 | 0.35 | 0.98 | 0.65 |
| Ni(200)/Pd(4)/Au(4) | 1.35 | 0.23 | 0.58 | 0.31 | 1.85 | 0.23 | 0.72 | 0.47 |
| Ni(200)/Pd(6)/Au(4) | 0.97 | 0.20 | 0.49 | 0.24 | 1.81 | 0.20 | 0.56 | 0.36 |
| Ni(200)/PdP(2)/Au(2) | 1.22 | 0.23 | 0.53 | 0.29 | 1.31 | 0.23 | 0.54 | 0.25 |
| Ni(200)/PdP(4)/Au(2) | 0.98 | 0.22 | 0.51 | 0.22 | 1.08 | 0.23 | 0.51 | 0.21 |
| Ni(200)/PdP(6)/Au(2) | 0.96 | 0.19 | 0.41 | 0.18 | 1.06 | 0.21 | 0.48 | 0.22 |
| Ni(200)/PdP(2)/Au(4) | 1.40 | 0.22 | 0.51 | 0.29 | 1.38 | 0.22 | 0.61 | 0.27 |
| Ni(200)/PdP(4)/Au(4) | 0.90 | 0.23 | 0.40 | 0.16 | 1.04 | 0.25 | 0.57 | 0.23 |
| Ni(200)/PdP(6)/Au(4) | 0.99 | 0.21 | 0.44 | 0.22 | 1.04 | 0.23 | 0.47 | 0.23 |

*Values in parentheses indicate the thickness (μin) of the respective metal layer; standard $t_{2/3} \leq 1$ s; no. of samples = 14; no. of pads per sample = 3

Table V. Ball shear strength and cold ball pull strength of ENEPIG-Pd and ENEPIG-PdP with varying thicknesses of Pd (or PdP) and Au layers

| System | Ball shear strength ^a (g) | | | | Cold ball pull strength ^b (g) | | | |
|----------------------|--------------------------------------|--------|--------|-----------|--|--------|--------|-----------|
| | Max. | Min. | Mean | Std. Dev. | Max. | Min. | Mean | Std. Dev. |
| Ni(200)/Pd(2)/Au(2)* | 1968.5 | 1701.8 | 1838.4 | 72.2 | 2358.2 | 1861.7 | 2065.0 | 147.1 |
| Ni(200)/Pd(4)/Au(2) | 1993.2 | 1704.9 | 1850.6 | 78.3 | 2399.7 | 1941.8 | 2119.7 | 116.9 |
| Ni(200)/Pd(6)/Au(2) | 1946.8 | 1686.6 | 1819.8 | 73.5 | 2335.4 | 1942.4 | 2127.0 | 99.8 |
| Ni(200)/Pd(2)/Au(4) | 1933.5 | 1644.8 | 1801.4 | 76.0 | 2240.9 | 1845.1 | 2048.9 | 110.7 |
| Ni(200)/Pd(4)/Au(4) | 1873.2 | 1601.3 | 1734.2 | 75.3 | 2342.5 | 1839.3 | 2085.8 | 111.0 |
| Ni(200)/Pd(6)/Au(4) | 1839.4 | 1583.5 | 1710.4 | 77.5 | 2303.6 | 1828.9 | 2058.9 | 134.2 |
| Ni(200)/PdP(2)/Au(2) | 1929.3 | 1548.6 | 1784.9 | 100.5 | 2247.2 | 1836.4 | 1988.1 | 92.3 |
| Ni(200)/PdP(4)/Au(2) | 1973.4 | 1632.7 | 1841.2 | 90.1 | 2246.9 | 1851.3 | 1977.0 | 99.3 |
| Ni(200)/PdP(6)/Au(2) | 1953.8 | 1641.9 | 1826.9 | 78.0 | 2214.2 | 1871.6 | 1971.5 | 84.8 |
| Ni(200)/PdP(2)/Au(4) | 1871.5 | 1556.6 | 1721.8 | 89.5 | 2143.8 | 1788.6 | 1956.7 | 94.9 |
| Ni(200)/PdP(4)/Au(4) | 1873.2 | 1668.7 | 1776.1 | 51.0 | 2164.9 | 1781.0 | 1886.7 | 101.0 |
| Ni(200)/PdP(6)/Au(4) | 1822.1 | 1586.4 | 1715.2 | 65.9 | 2192.1 | 1771.5 | 1914.4 | 123.5 |

*Values in parentheses indicate the thickness (μin) of the respective metal layer; ^aStandard shear force > 1000 g; no. of samples = 15; no. of balls per sample = 8; ^bno. of sample = 5; no. of balls per sample = 8

the corresponding samples that were aged with no reflow. This would mean that the samples with a 2- μin Au layer did not have uniform wire-bonding capacities.

In Fig. 7, the wire bond pull strength data for ENEPIG-Pd and ENEPIG-PdP with a 4- μin Au layer and varying thickness of Pd or PdP layer and reflow time are presented. For the ENEPIG-Pd samples, the ranges of wire bond pull strength were wider than those for the ENEPIG-PdP samples. However, it is quite interesting to note that only the ENEPIG-PdP samples with a 4- μin or 6- μin PdP layer had the narrowest ranges, which is favorable because, for these samples, the wire-bonding

capacity could be uniform. The ENEPIG-Pd samples that were aged with 2× reflow had a wider range of wire bond pull strength than the corresponding samples that were aged with no reflow.

Surface Morphology

The SEM images in Figs. 8–10 show the surface characteristics of different ENEPIG samples. The surfaces of the ENEPIG-Pd samples with a 2- μin or 4- μin Au layer (Figs. 8) show some (degree of) roughness, with black voids (encircled in the images). The surfaces of the ENEPIG-PdP samples were generally smoother compared with those of the

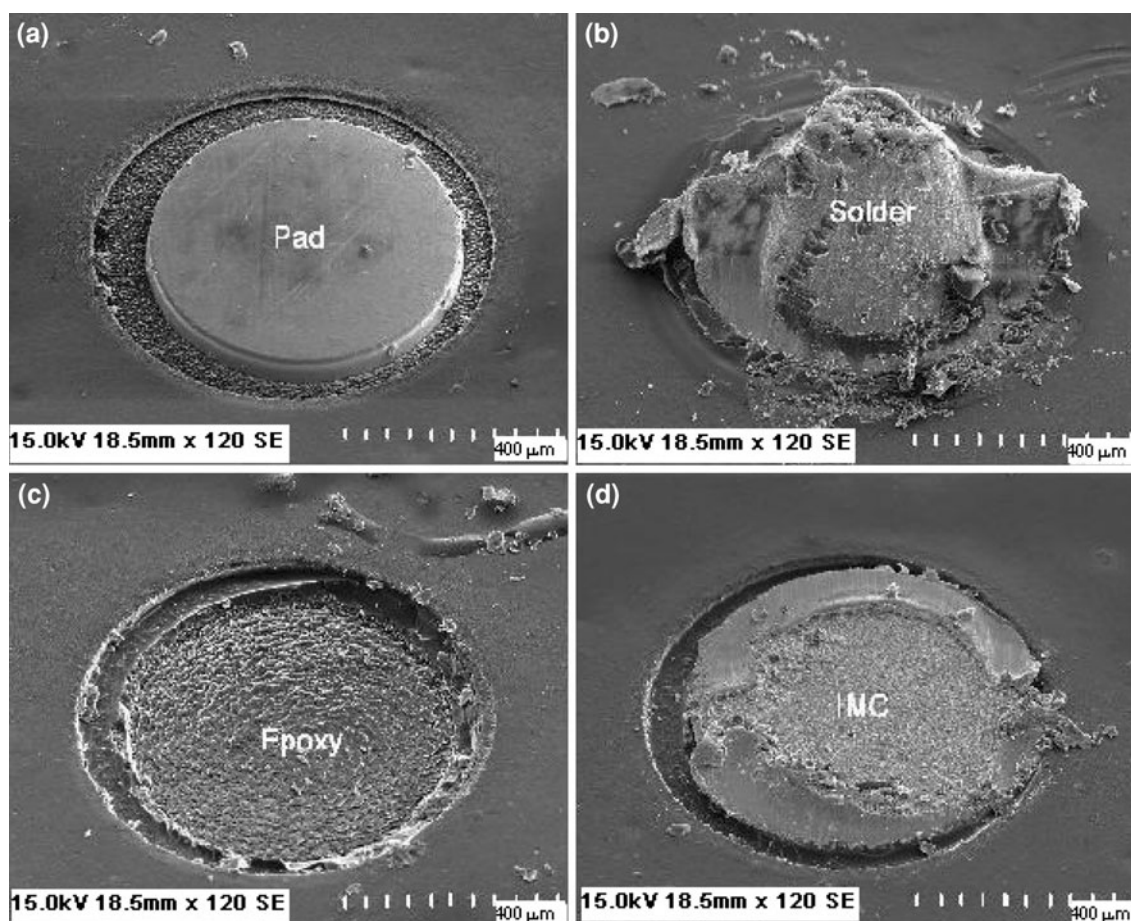


Fig. 3. Cold ball pull failure modes: (a) pad before test, (b) ball failure mode, (c) pad failure mode, and (d) bond failure mode.

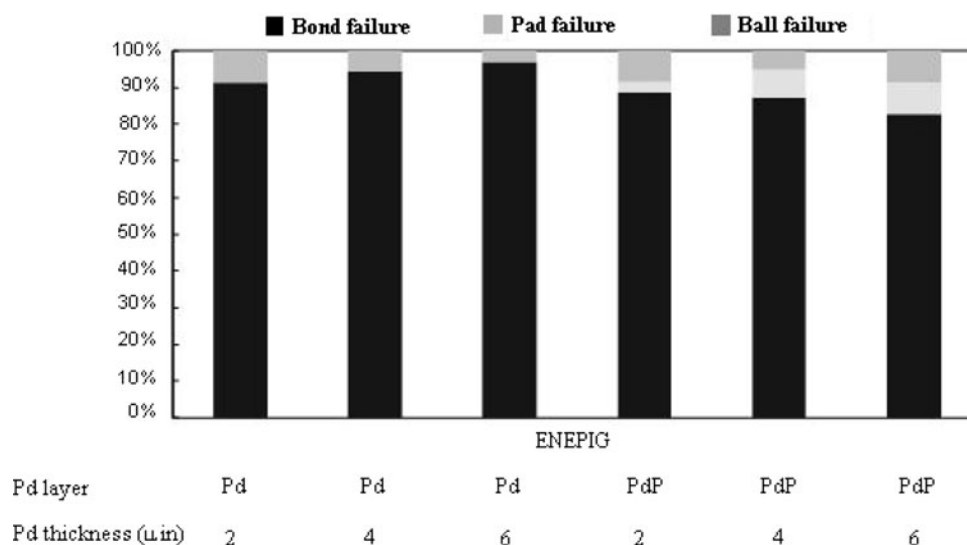


Fig. 4. Comparison of cold ball pull failure mode results for ENEPIG-Pd with ENEPIG-PdP with 2-μin Au layer and varying thickness of Pd layer.

ENEPIG-Pd samples; there were no black voids observed. These observations were upheld further when the Au layers were stripped off the surface of the samples, and the resulting surface was

photographed with SEM. Resulting images are shown in Figs. 9 and 10. Cracks were observed on the surfaces of the ENEPIG-Pd samples with a 2-μin or 4-μin Au layer (that had been stripped off).

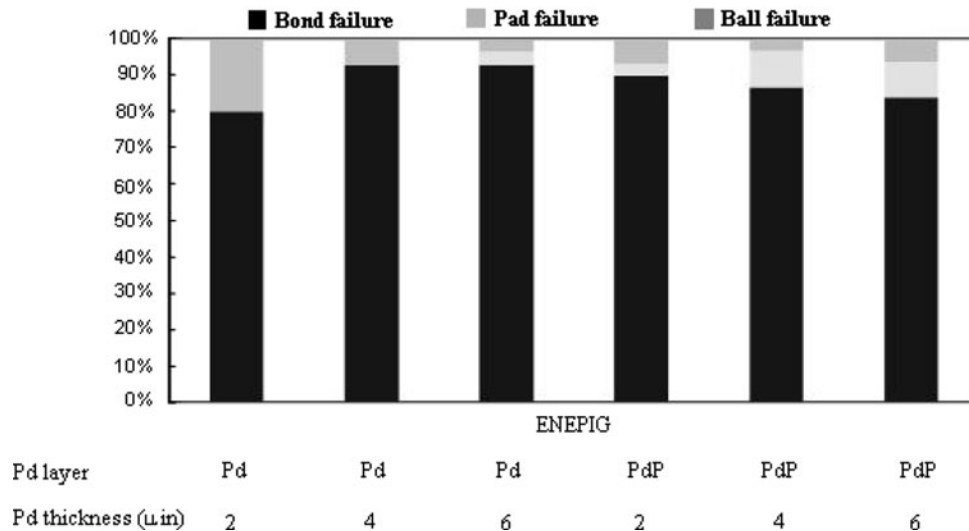


Fig. 5. Comparison of cold ball pull failure mode results for ENEPIG–Pd with ENEPIG–PdP with 4-μin Au layer and varying thickness of Pd layer.

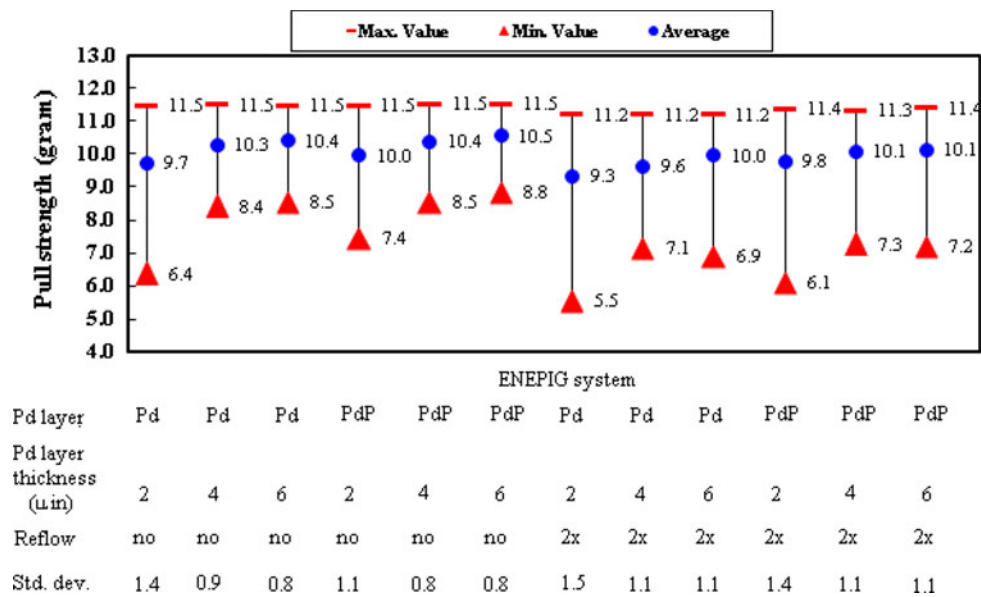


Fig. 6. Comparison of wire bond pull strength of ENEPIG–Pd with ENEPIG–PdP with 2-μin Au layer and varying thickness of Pd layer and reflow time.

These cracks could be associated with the black voids that had been observed on the surface before stripping the gold layer off. The presence of such cracks (mud cracks) has been identified as an indicator of corrosion of the Ni layer surface (black pad defect) in metal surface finishes.^{2,14,15} The concentration of cracks decreased with the increase in the Pd layer thickness. In the ENEPIG–PdP samples, cracks, which are fewer in number compared with those in the ENEPIG–Pd samples, were observed

only on the surface of the sample with a 2-μin PdP layer. As shown in Figs. 9 and 10, the cracks completely disappeared as the PdP layer thickness was increased to 4-μin and then further to 6-μin. Such results can be attributed to the amorphous PdP layer present between the Au and electroless nickel layers, which has been reported to prevent galvanic attack on the nickel layer brought about by the immersion Au plating process.¹³ Since these cracks (or black voids) could be associated with the

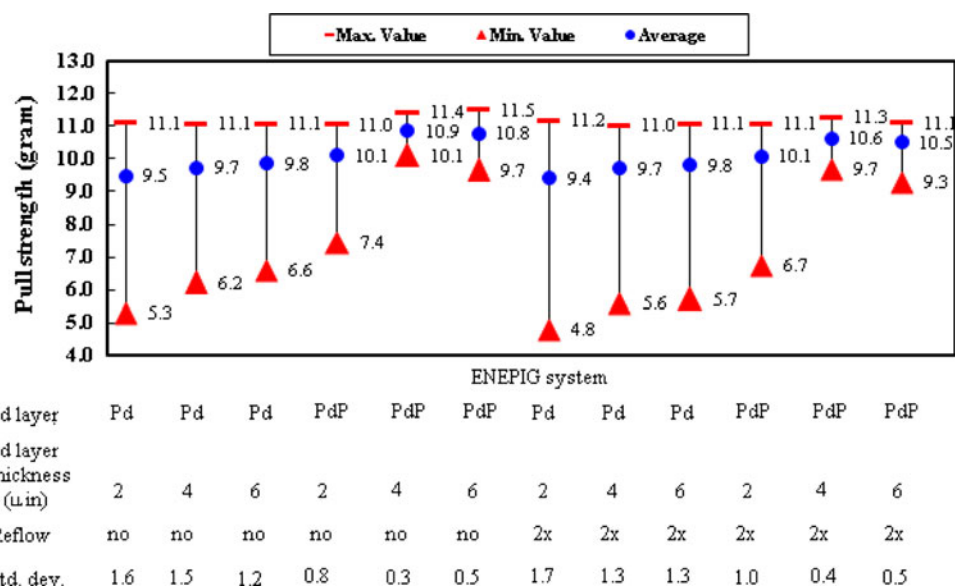


Fig. 7. Comparison of wire bond pull strength of ENEPIG-Pd with ENEPIG-PdP with 4- μ m Au layer and varying thickness of Pd layer and reflow time.

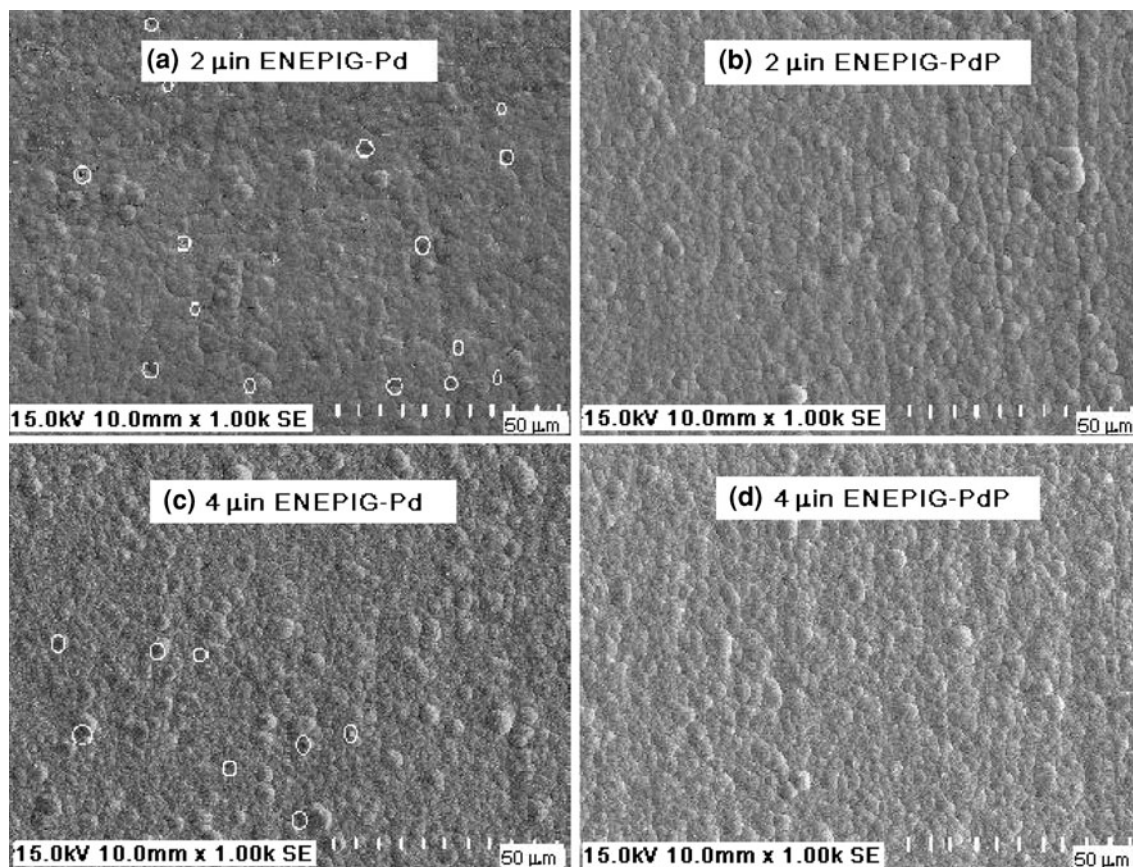


Fig. 8. SEM images of ENEPIG surfaces with 2- μ m Au layer and (a) 2- μ m Pd layer or (b) 2- μ m PdP layer; ENEPIG surfaces with 4- μ m Au layer and (c) 4- μ m Pd layer or (d) 4- μ m PdP layer.

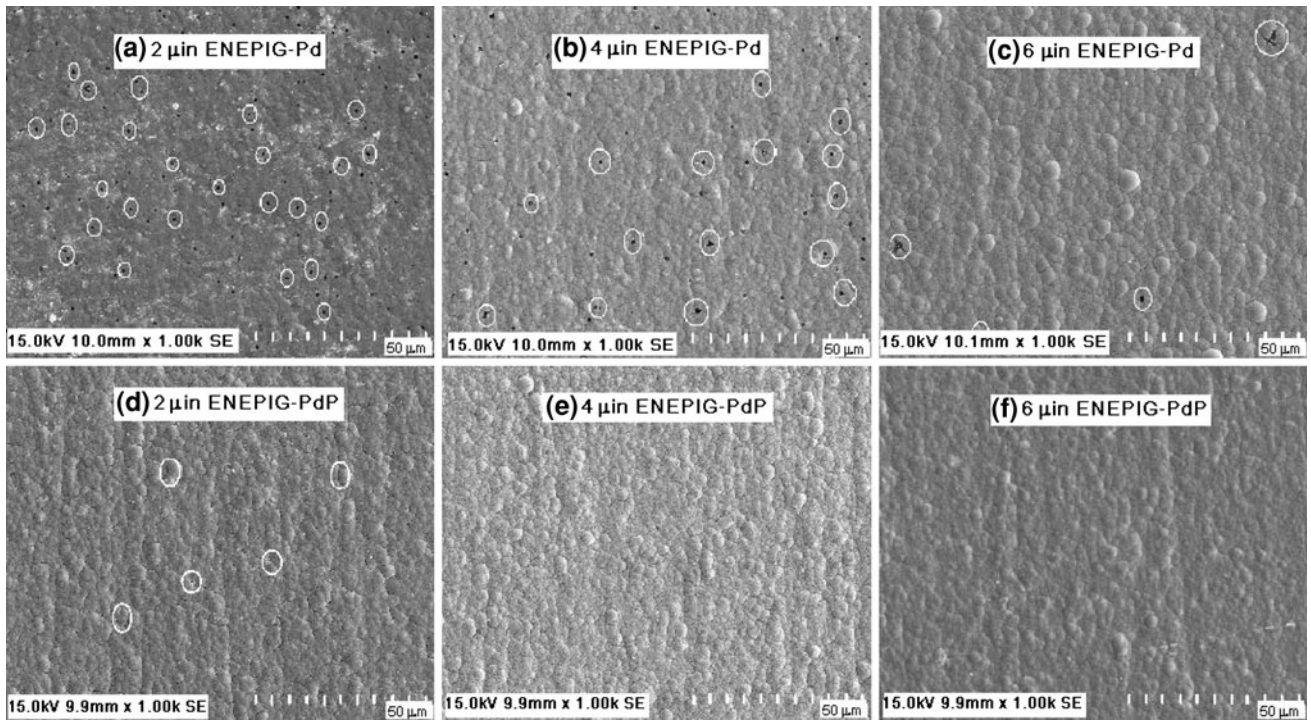


Fig. 9. SEM images of ENEPIG surfaces with 2-μm Au layer after removing the Au layer: (a) ENEPIG with 2-μm Pd layer, (b) ENEPIG with 4-μm Pd layer, (c) ENEPIG with 6-μm Pd layer, (d) ENEPIG with 2-μm PdP layer, (e) ENEPIG with 4-μm PdP layer, (f) ENEPIG with 6-μm PdP layer.

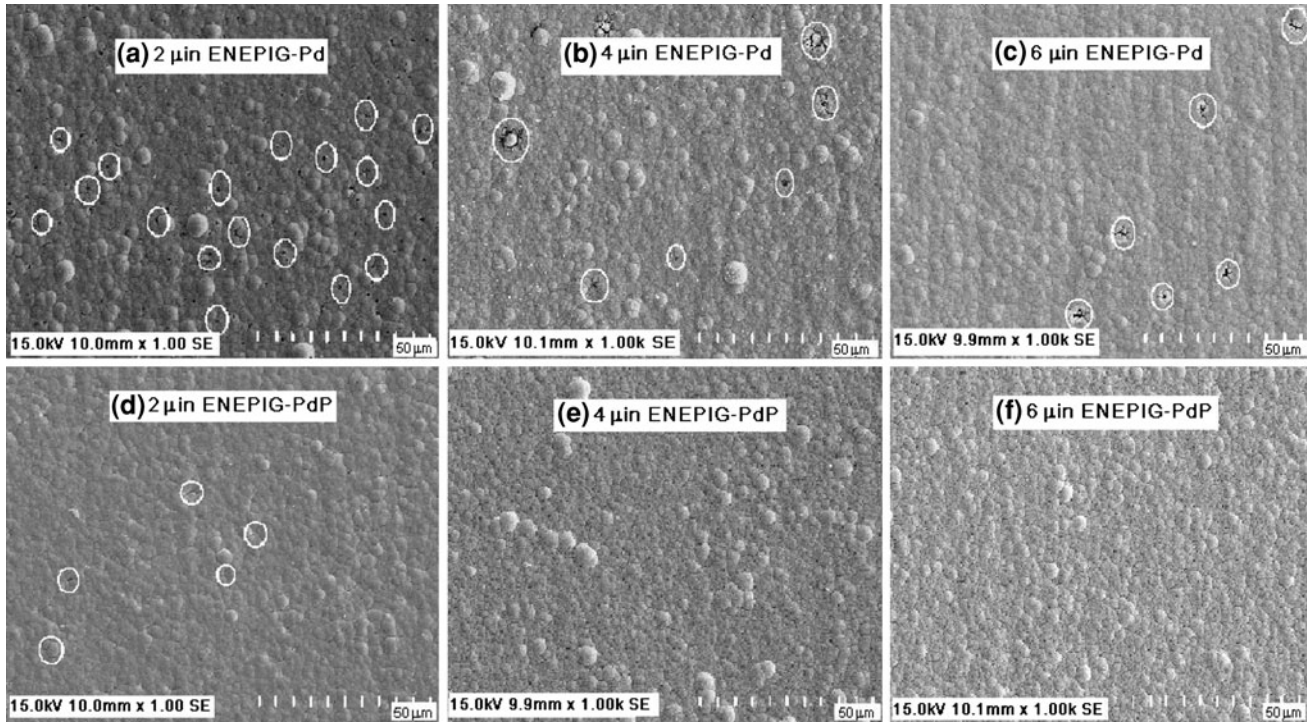


Fig. 10. SEM images of ENEPIG surfaces with 2-μm Au layer after removing the Au layer: (a) ENEPIG with 2-μm Pd layer, (b) ENEPIG with 4-μm Pd layer, (c) ENEPIG with 6-μm Pd layer, (d) ENEPIG with 2-μm PdP layer, (e) ENEPIG with 4-μm PdP layer, (f) ENEPIG with 6-μm PdP layer.

susceptibility of the metal surface finish to corrosion, this is an indication that, as the Pd or PdP layer thickness increases, the surface would become more resistant to corrosion. Also, in this particular case, the presence of P in the Pd layer makes the metal finish more resistant to corrosion.

CONCLUSIONS

Although both ENEPIG–Pd and ENEPIG–PdP samples tested passed the wettability tests, it was found that the ENEPIG–Pd samples exhibited relatively better wetting time and wetting force. Likewise, the mechanical strength of the ENEPIG–Pd samples was, in general, relatively better than that of ENEPIG–PdP samples, although, when it came to consistency in wire bonding strength values, the ENEPIG–PdP samples with a 4- μin or 6- μin PdP layer were the best and hence are most preferred. Results of SEM performed to examine the surface characteristics of the pads suggested that the ENEPIG pad sample with a 4- μin -thick Au layer and 4- μin -thick PdP layer possessed stable wire-bonding capacity and excellent lead-free solder reliability.

ACKNOWLEDGEMENTS

This research was supported by an industry grant from OMG (Asia) Electronic Chemicals Company, Ltd. and a Grant, NSC 99-2221-E-033-044-MY3, from the National Science Council of the Republic of China.

REFERENCES

1. Y. Oda, M. Kiso, S. Kurosaka, A. Okada, K. Kitajima, S. Hashimoto, and D. Gudczasuskas (Proceedings of the 41st International Symposium on Microelectronics (IMAPS), Rhode Island, U.S.A., 2008).
2. K. Zeng, R. Stierman, D. Abbott, and M. Murtuza, *JOM* 58, 75 (2006).
3. Y.S. Won, S.S. Park, J. Lee, J.-Y. Kim, and S.-J. Lee, *Appl. Surf. Sci.* 257, 56 (2010).
4. X. Huang, S.W.R. Lee, L. Ming, and W.T. Chen, *IEEE Trans. Electron. Packag. Manuf.* 31, 185 (2008).
5. P. Ratchev, S. Stoukatch, and B. Swinnen, *Microelectron. Reliab.* 46, 1315 (2006).
6. G. Milad and M. Orduz, *Metal Finish.* 105, 25 (2007).
7. Y. Kim, J.-Y. Park, and Y.-H. Kim, *J. Electron. Mater.* 41, 763 (2012).
8. W.H. Wu, C.S. Lin, S.H. Huang, and C.E. Ho, *J. Electron. Mater.* 39, 2387 (2010).
9. A.J.G. Strandjord, S. Popelar, and C. Jauernig, *Microelectron. Reliab.* 42, 265 (2002).
10. J.W. Yoon, B.I. Noh, and S.B. Jung, *J. Electron. Mater.* 40, 1950 (2011).
11. C. Faure and J. Bath, *Lead-Free Soldering* (New York: Springer, 2007).
12. M. Oezkoek, H. Roberts, and J. McGurran (Proceedings of the 43rd International Symposium on Microelectronics (IMAPS), North Carolina, U.S.A., 2010).
13. C.E. Ho, W.H. Wu, C.C. Wang, and Y.C. Lin, *J. Electron. Mater.* 41, 3266 (2012).
14. K. Zeng, R. Stierman, D. Abbott, and M. Murtuza (Proceedings of Tenth Intersociety Conference on Thermal and Thermomechanical Phenomena in Electronics Systems (ITHERM), San Diego, CA, IEEE, New York, U.S.A., 2006), p. 1111.
15. N. Biunno and M. Barbetta (Proceedings of Surface Mounting Technology International, San Jose, California, SMTA, Edina, MN, 1999), p. 561.